Enhancement of carrier lifetimes in type-II quantum dot/quantum well hybrid structures

O. D. D. Couto, Jr.,[1,a)] P. T. de Almeida,[1] G. E. dos Santos,[1] M. A. G. Balanta,[1] H. F. Andriolo,[1] J. A. Brum,[1] M. J. S. P. Brasil,[1] F. Iikawa,[1] B. L. Liang,[2,b)] and D. L. Huffaker[2]
[1]*Instituto de Física "Gleb Wataghin," Universidade Estadual de Campinas, 13083-859 Campinas, São Paulo, Brazil*
[2]*California NanoSystems Institute, UCLA, Los Angeles, California 90095, USA*

(Received 8 June 2016; accepted 11 August 2016; published online 25 August 2016)

We investigate optical transitions and carrier dynamics in hybrid structures containing type-I GaAs/AlGaAs quantum wells (QWs) and type-II GaSb/AlGaAs quantum dots (QDs). We show that the optical recombination of photocreated electrons confined in the QWs with holes in the QDs and wetting layer can be modified according to the QW/QD spatial separation. In particular, for low spacer thicknesses, the QW optical emission can be suppressed due to the transference of holes from the QW to the GaSb layer, favoring the optical recombination of spatially separated carriers, which can be useful for optical memory and solar cell applications. Time-resolved photoluminescence (PL) measurements reveal non-exponential recombination dynamics. We demonstrate that the PL transients can only be quantitatively described by considering both linear and quadratic terms of the carrier density in the bimolecular recombination approximation for type-II semiconductor nanostructures. We extract long exciton lifetimes from 700 ns to 5 μs for QDs depending on the spacer layer thickness. *Published by AIP Publishing.* [http://dx.doi.org/10.1063/1.4961534]

I. INTRODUCTION

Type-II self-assembled quantum dots (QDs) offer a unique perspective for wavefunction engineering towards device applications. By exploring carrier and spin dynamics via control of quantum confinement properties in this type of nanostructure, new functionalities and applications are expected to be demonstrated, especially in fields like quantum information processing.[1,2] In particular, the staggered type-II band alignment of GaSb/GaAs heterostructures also offers new possibilities for fundamental physics research. GaSb QDs embedded in GaAs matrixes are characterized by the spatial separation of electrons and holes and a strong hole localization.[3,4] From the device application perspective, GaSb/GaAs QDs have been employed in solar cell experiments,[5–8] laser devices,[9,10] and strong hole localization has created interesting perspectives for efficient charge-based memory devices.[11,12] From the fundamental point of view, carrier dynamics in this system started to be investigated around two decades ago.[13–16] However, recent optical spectroscopy experiments[17–20] have led to a deeper understanding of its main features and even led to the suggestion of a breakdown of the bimolecular recombination (BR) approximation for this system.[21]

The controlled type-II coupling between different nanostructured systems offers an additional degree of freedom in order to explore carrier dynamics in benefit of applications. In type-I systems, the coupling between quantum wells (QWs) and QDs has thoroughly been studied regarding its carrier[22–26] and spin properties.[27] In type-II QW+QD systems, however, few optical spectroscopy studies have been performed.[17,19,28] Its interest has been renewed, especially after the recent demonstration of solar cells based on type-II QW+QD systems which are more efficient with respect to those where either QWs or QDs were employed.[29,30]

In this work, we analyse the optical properties of GaSb QDs coupled to GaAs QWs via a variable width AlGaAs spacer. Using continuous wave (CW) photoluminescence (PL) and photoluminescence excitation (PLE) measurements, we demonstrate that, for barrier thicknesses below 10 nm, the optical emissions from GaSb QDs and wetting layer (WL) dominate and the QW emission is drastically reduced due to the escape of holes from the QW to the GaSb layer. In contrary to what is usually assumed, time-resolved (TR) PL measurements show that recombination rates are not proportional to the carrier density, thus leading to non-exponential time-transients which change with barrier thickness and are strongly dependent on the initial carrier concentration pumped into the system. By varying laser power for more than two orders of magnitude, we show that the carrier dynamics can only be satisfactorily described by taking into account all terms in the BR approximation for recombination rates, i.e., both linear and quadratic terms of the photocreated carrier density. Using this model, we obtain carrier lifetimes of up to 5 μs for GaSb QDs, which are considerably longer than the reported values for GaSb/GaAs QDs.[13,15,17,19,31] Our results keep alive the discussion about the BR approximation validity reported by Hodgson *et al.*[21]

II. EXPERIMENTAL

Our hybrid QW/QD structures were grown using a solid-source molecular beam epitaxy reactor on semi-insulating GaAs (100) substrates after the deposition of a 200 nm GaAs buffer layer and a 70 nm $Al_{0.3}Ga_{0.7}As$ barrier at 580 °C. The

[a)]Electronic address: odilon@ifi.unicamp.br
[b)]Electronic address: bliang@cnsi.ucla.edu

hybrid structure consists of a 5 nm GaAs QW, an $Al_{0.3}Ga_{0.7}As$ spacer of variable thickness (d), and a single layer of self-assembled GaSb QDs as depicted in Figure 1(a). Samples A, B, and C have values of $d = 10$, 5, and 2 nm, respectively. The QDs were formed for all samples by deposition of 3.2 ML of GaSb at 490 °C with a Ga growth rate of 0.18 ML/s and a Sb/Ga beam equivalent pressure ratio of 1.2. After QD formation, the GaSb QD layer was capped by 10 nm $Al_{0.3}Ga_{0.7}As$ at 490 °C and then 60 nm $Al_{0.3}Ga_{0.7}As$ at 540 °C. Finally, 5 nm GaAs was grown on top to avoid oxidation of the $Al_{0.3}Ga_{0.7}As$ layer. A reference sample containing a single layer of GaSb/AlGaAs QDs was grown under the same conditions.

Macro-PL measurements were performed with a solid-state laser at 532 nm and low temperatures were achieved with a He-flux cryostat. Emission was analysed using a single spectrometer with a photomultiplier. PLE measurements were done with a wavelength tunable Ti:Saph CW laser and a double monochromator equipped with a photomultiplier. In CW μ-PL measurements, excitation was performed with the same 532 nm solid state laser and lower temperatures were achieved with a cold-finger He cryostat. An objective lens focused the laser down to a spot size $\approx 2\,\mu$m. Sample emission was analysed with a single spectrometer equipped with a 1200 gr/mm optical grating and a CCD camera. TR μ-PL measurements were performed with the same cold-finger He cryostat and objective lens. A pulsed diode laser emitting at 405 nm (0.5 ns pulse width) was used as the excitation source. Repetition rates of 100 and 200 kHz were employed. A streak camera was used to record the PL emission as a function of time. All measurements were performed at 10 K.

III. RESULTS AND DISCUSSION

Figure 1(b) shows the potential profiles of the conduction band (CB) and valence band (VB) edges along the growth direction and the 3 optical transitions due to quantum confinement which are expected to dominate the PL spectra of samples A, B, and C. The type-I (spatially direct) transition between electrons and holes in the GaAs QW (labeled E^D_{QW}) is expected be more efficient for larger values of the AlGaAs spacer d. As spacer thickness decreases, two lower energy type-II (spatially indirect) transitions are expected to occur. E^I_{WL} is the transition between an electron in the GaAs QW and a hole in the GaSb WL, while in E^I_{QD} the hole is situated in the GaSb QD. E^I_{QD} should be the lowest energy transition.

Figures 2(a), 2(b), 2(c), and 2(d) show macro-PL and PLE measurements for the reference sample, samples A, B, and C, respectively. The PL spectrum of the reference sample is characterized by a broad emission band at ≈ 1.69 eV which occurs due the recombination of electrons in the AlGaAs barriers and holes in the GaSb WL [we label it E^{I*}_{WL}]. The QD emission peak (E^{I*}_{QD}) is not visible in this measurement because it is hindered by the strong emission from the GaAs substrate and buffer layer (3 peaks between 1.45 and 1.52 eV corresponding to bound-exciton, donor-acceptor (D-A), and its optical phonon replica transitions). E^{I*}_{QD} can

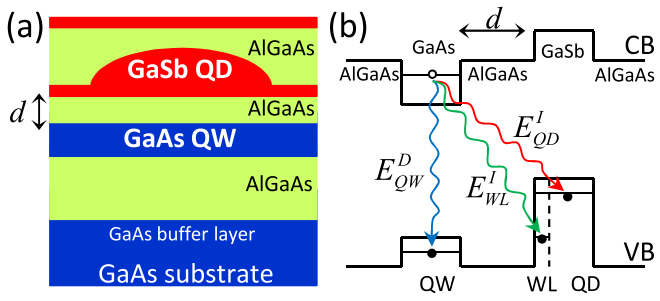

FIG. 1. (a) Hybrid QW/QD system coupled by a spacer layer of thickness d. (b) Band-alignment scheme and optical transitions expected for samples A, B, and C.

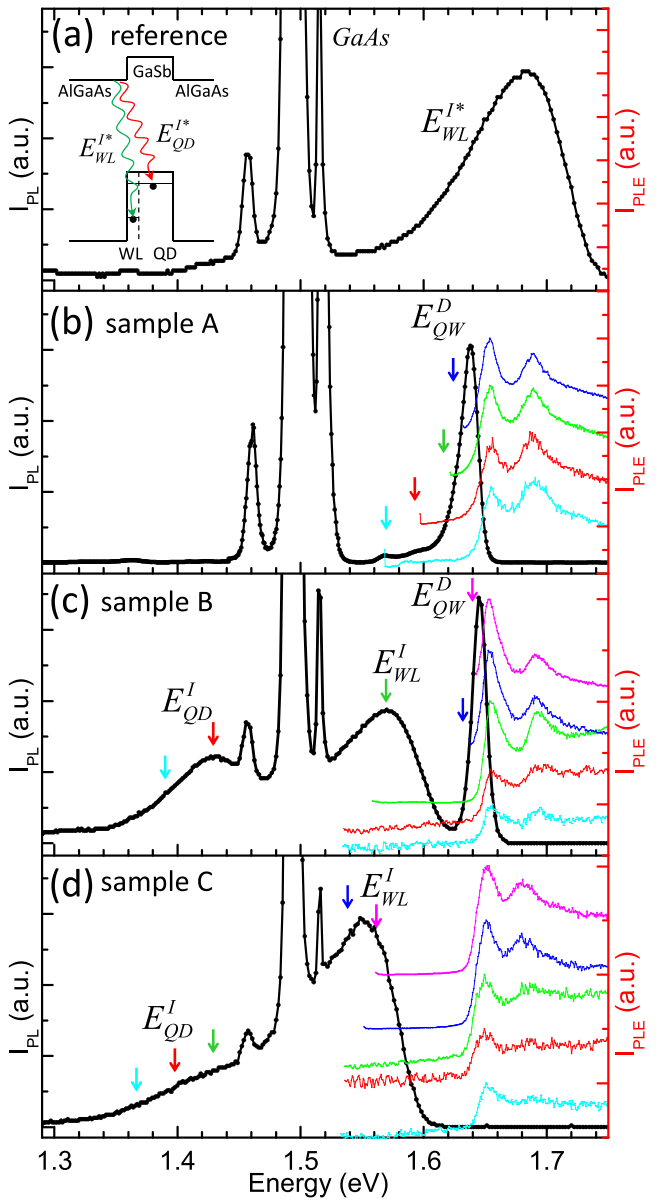

FIG. 2. From top to bottom: macro-PL (black dotted spectra) and PLE (coloured lines) for the (a) reference sample (the inset shows the potential profile and the optical transitions expected for this sample), (b) sample A ($d = 10$ nm), (c) sample B ($d = 5$ nm), and (d) sample C ($d = 2$ nm). The GaAs related peaks are saturated in all PL spectra to make the other optical transitions more evident. Arrows indicate the positions where PLE was detected.

be clearly observed for temperatures above 30 K (not shown) when GaAs-related emissions quench.

For sample A, the 10 nm separation between QDs and QWs makes PL emission mainly dominated by the narrow E^D_{QW} emission at 1.63 eV. The thicker barrier makes E^I_{QD} and E^I_{WL} very weak. The two well defined peaks observed for the PLE spectra detected at different energies shown in Figure 2(b) are attributed to the heavy and light-hole free exciton states of the QWs. The weak feature observed at ≈1.59 eV slightly below the E^D_{QW} peak is also attributed to the GaAs QW. Its lower energy is due to the tensile strain induced by the GaSb QDs. A similar effect was observed in previous works using self-assembled QDs as stressors to produce localized states in a QW.[32,33] The energy shift of ≈50 meV is a typical value obtained for this kind of structure. The PLE spectrum obtained for a detection energy fixed at 1.58 eV [cyan curve in Figure 2(b)] is similar to that obtained at 1.63 eV, which indicates the link of this emission to the QW.

The PL spectrum of sample B ($d = 5$ nm) shown in Figure 2(c) is significantly different from sample A. Now, the increase in the electron-hole wavefunction overlap contributes to increase the efficiency of the indirect transitions E^I_{QD} and E^I_{WL}. In fact, both peaks show similar intensities to E^D_{QW}. PLE spectra detected at E^I_{WL} (green PLE curve) and E^D_{QW} (red and cyan curves) demonstrate the hole injection from the QW into WL and QD structures. The same behavior is observed in Figure 2(d) for sample C. In this case, however, the proximity between QWs and QDs makes hole tunneling to the WL and QDs more efficient than recombination with electrons in the QW, thus leading to the vanishing of the E^D_{QW} peak. PLE spectra detected at QD emission energies on samples B and C [cyan and red PLE spectra in Figures 2(c) and 2(d)] suggest that hole injection from the WL into the QDs is less efficient than injection from the QW, thus indicating that localized states contribute significantly to WL emission. The fact that holes cannot easily relax from the WL to QDs is the reason for a relatively high PL intensity of the WL emission in samples B and C.

Figure 3(a) shows the μ-PL spectra of sample B as a function of the excitation power. As we observe, the indirect PL emissions (E^I_{QD} and E^I_{WL}) blueshift with power while E^D_{QW} stays almost unchanged. This is summarized in Figure 3(b), where we see that blueshifts (ΔE) reach approximately 40 meV for the indirect emission at elevated powers. The inset presents the result for E^I_{WL} in sample C, which is very similar. The PL blueshift in type-II GaSb/GaAs QDs has been observed in a couple of previous experimental works. However, its origin (including the blueshift in other type-II QDs) is still a source of debate. In general, three main effects related to carrier accumulation are mentioned as causes of the large PL blueshift in type-II QDs: (i) band-bending;[13–15] (ii) capacitive-charging;[17,34–36] and (iii) state-filling.[16] All these effects rely on the assumption of the BR model. However, Hodgson and his co-workers recently suggested a possible breakdown of the BR approximation for this type of system.[21] In order to further investigate this problem, we performed μ-PL TR experiments in our samples.

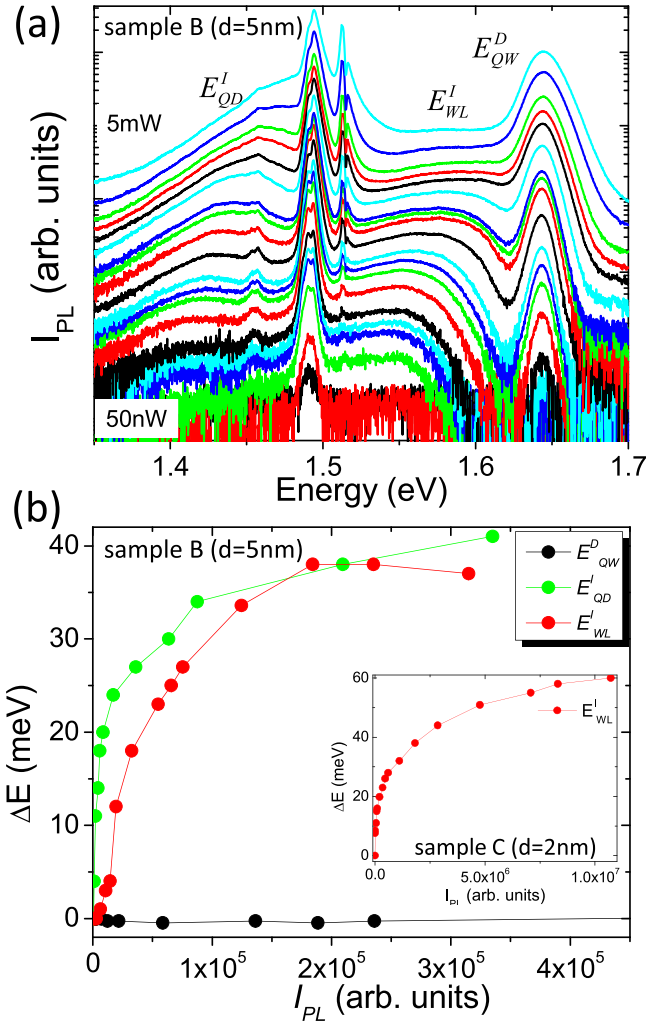

FIG. 3. (a) CW μ-PL from sample B as a function of excitation power. (b) Peak position of the three main emissions (E^D_{QW}, E^I_{QD}, and E^I_{WL}) as a function of the PL emission intensity extracted from the spectra in (a). The inset shows the dependence of E^I_{WL} with I_{PL} for sample C.

Figure 4 summarizes the TR μ-PL measurements for sample C. The dots in Figures 4(a) and 4(b) represent, respectively, the experimental data for E^I_{WL} and E^I_{QD} emissions measured at the lowest average excitation power (10 nW at 200 kHz). The inset in Figure 4(a) presents the streak-camera image in the spectral region of E^I_{WL} obtained for 10 nW power. The time transient in the main plot is obtained after integration of this image between 790 and 810 nm approximately. Figures 4(c) and 4(d) show transients for the same emissions at the highest average power delivered by our diode-laser (3 μW at 200 kHz). The major feature observed in the experimental data is the fact that all decay profiles are clearly non-exponential (note the logarithm vertical scales for I_{PL}). Non-exponential decays have already been observed experimentally for this type of structure,[13,15,17,19,31] but they have usually been fitted with two exponential curves, thus assuming that $I_{PL}(t)$ is always proportional to the excess carrier density $\Delta n(t)$ created after optical excitation. The two-exponential approach is adopted on the assumption that the electron-hole wavefunction overlap changes during the carrier relaxation process. In this way, a faster decay time (τ_1) is associated with the regime where QDs

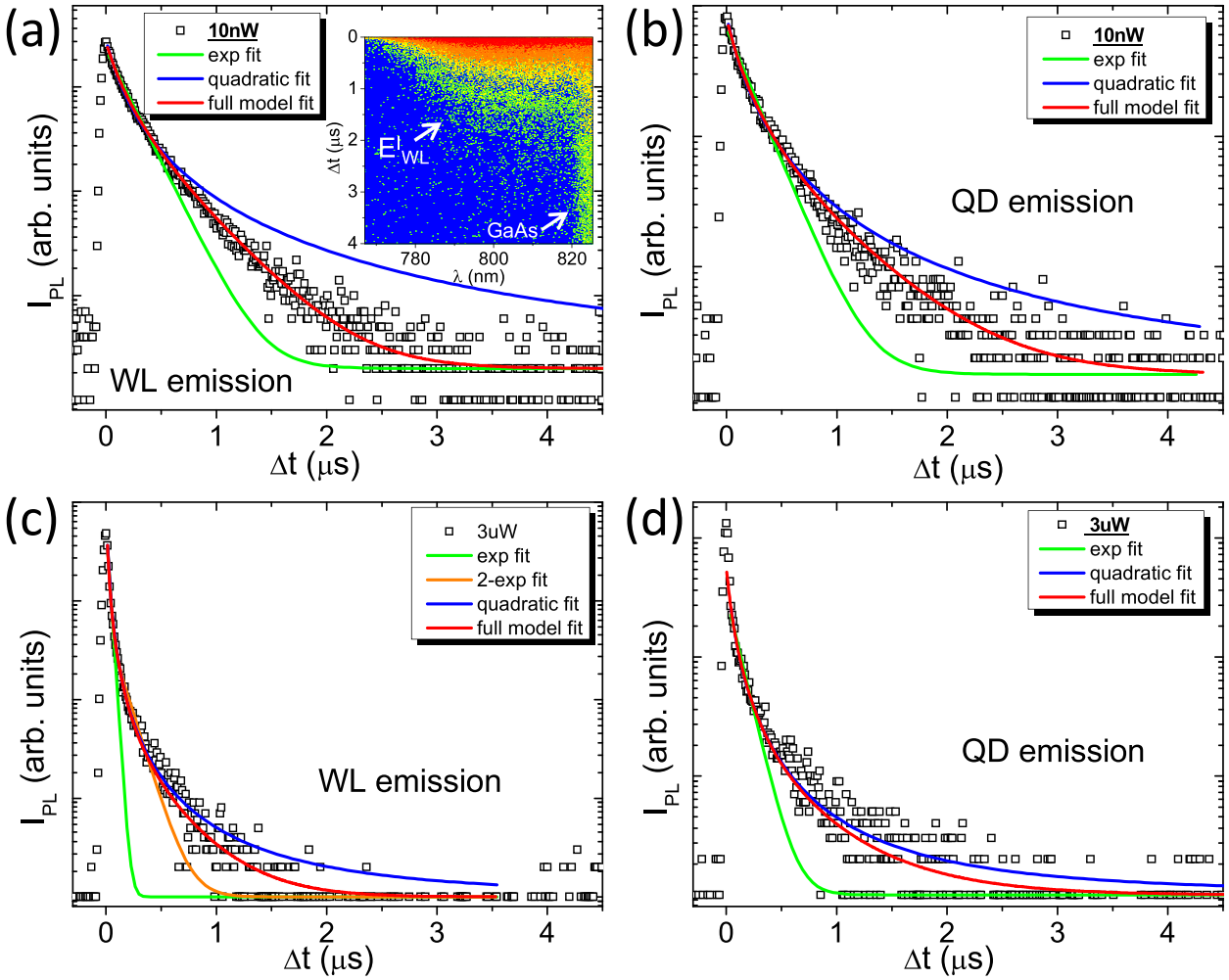

FIG. 4. PL time transients for sample C. At low excitation power (10 nW): (a) WL and (b) QD emissions, respectively. At high power (3 μW): (c) WL and (d) QD emissions, respectively. Solid lines represent fittings with Equations (4) (green), (5) (blue), and (6) (red). The orange solid line in (c) is a fit with two-exponential time constants (τ_1 and τ_2). The inset in (a) shows the time dependence of the PL signal for E^I_{WL} measured at 10 nW. The GaAs D-A recombination is indicated by an arrow. The transient in (a) is obtained by integration of this image from 790 to 810 nm.

and WL have a high density of carriers, when a high wavefunction overlap caused by carrier accumulation immediately after laser pulse excitation is supposed to happen. A slower decay time (τ_2) is, therefore, associated with the regime where QDs have one or less than one exciton/dot so that the wavefunction overlap is reduced and reflects simply the spatial separation of electrons and holes.[13,15,19] In Ref. 15, for example, it is very clear how the two-exponential fit is not able to reproduce accurately the curved behaviour of the decay profiles. We have also tried to fit our data with one and two exponentials, but the results were neither consistent nor satisfactory.

In order to reproduce accurately the experimental results, we need to take into account all terms in $\Delta n(t)$ expected from the BR approximation, which is commonly invoked to describe carrier dynamics in type-II quantum dots.[15,21,37] In such a model,[38] also known as Langevin model,[39] the carrier recombination rate equation is given by law of mass action

$$R = Bnp, \tag{1}$$

where B is the recombination coefficient, which is determined by the electron-hole wavefunction overlap, and n and p are the electron and hole concentrations, respectively.

Based on the PL and PLE results discussed above, we can consider QW-WL and QW-QD recombinations as decoupled, which allows us to write independent rate equations for them. We also assume that electrons and holes are thermalized prior to recombination. In this way, after a pulsed optical excitation, in any of the two recombination channels, the electron and hole concentrations in the system can be written as $n(t) = n_0 + \Delta n(t)$ and $p(t) = p_0 + \Delta p(t)$, respectively, where n_0 and p_0 are the equilibrium electron and hole concentrations. Assuming that $\Delta n(t) = \Delta p(t)$, Equation (1) can be written as

$$\begin{aligned} R(t) &= Bn_0p_0 + B(n_0 + p_0)\Delta n(t) + B\Delta n^2(t), \\ R(t) &= R_0 + R_{ex}(t). \end{aligned} \tag{2}$$

The first term in Equation (2) [$R_0 = Bn_0p_0$] is the equilibrium carrier recombination rate associated with non-zero temperatures. After the generation of a population of carriers at time $t = 0$, the excess carrier recombination rate [$R_{ex}(t)$], which is proportional to the PL intensity, is determined by the rate equation

$$\frac{d\Delta n(t)}{dt} = -R_{ex}(t) = -B(n_0 + p_0)\Delta n(t) - B\Delta n^2(t). \tag{3}$$

Assuming that B does not change with time, in the low carrier density limit $[\Delta n(t) \ll (n_0 + p_0)]$, the last term in Equation (3) can be neglected, thus leading to the usual exponential decay for carrier recombination, i.e.,

$$I_{PL}(t) = I_0 e^{-t/\tau}, \tag{4}$$

where the carrier lifetime $\tau = 1/B(n_0 + p_0)$ and $I_0 \propto B(n_0 + p_0)\Delta n_0$, with $\Delta n_0 = \Delta n(t = 0)$ been the initial carrier concentration. In this way, exponential decays for carrier relaxation dynamics are expected only in cases where carrier density is low ($I_{PL}(t) \propto \Delta n(t)$) and wavefunction overlap (B) is constant, which contradicts the arguments of the usual two-exponential approach where two decays in the form of Equation (4) (with decays constants τ_1 and τ_2) are used to fit the experimental data.[13,15,17,19,31]

If the excess carrier density is high $[\Delta n(t) \gg (n_0 + p_0)]$, the first term on the right side of Equation (3) can be neglected. This usually happens for short times immediately after the laser pulse. In this situation, the time dependence of the PL intensity can be approximated by

$$I_{PL}(t) = \frac{I_0}{\left[1 + \frac{t}{\tau_Q}\right]^2}, \tag{5}$$

where $I_0 \propto B\Delta n_0^2$. Here, we define $\tau_Q = 1/B\Delta n_0$ as a phenomenological decay constant since for this situation, the decay constant changes with time.[38] According to Equation (5), PL decay is expected to be non-exponential. This high carrier density approximation assumes that $I_{PL}(t) \propto \Delta n^2(t)$. It is only valid, however, for short times after laser excitation. When the carrier density becomes low enough, the first term in Equation (3) has to be taken into account.

The appropriate way to describe carrier dynamics is, therefore, to solve Equation (3) considering both linear and quadratic terms. The solution is analytical and has the form

$$I_{PL}(t) = I_0 \frac{A}{e^{t/\tau} - A}\left[1 + \frac{A}{e^{t/\tau} - A}\right], \tag{6}$$

where again the phenomenological decay constant is given by $\tau = 1/B(n_0 + p_0)$ [as in Equation (4)] and $I_0 \propto B(n_0 + p_0)^2$.

The parameter A is related to the ratio between the initial carrier concentration (Δn_0) and the residual carrier density ($n_0 + p_0$) by

$$\frac{\Delta n_0}{n_0 + p_0} = \frac{A}{1 - A}. \tag{7}$$

The solid green, blue, and red lines in Figure 4(a) were obtained by fitting the experimental data with Equations (4) and (5) (which we call quadratic), and (6) for the WL emission in sample C, respectively. The green line fit shows that, even for the lowest average power we could detect reasonable PL signal, the system is not in the linear recombination regime yet (Equation (4)). The blue curve demonstrates that the quadratic fit alone describes carrier dynamics only during the first 400 ns after laser pulse, overestimating the carrier population for longer times. A very good agreement, however, is found by fitting the experimental data with Equation (6). The same result is obtained for the QD decay profile shown in Figure 4(b). For this excitation power, we estimate a carrier density of around 10^{10}–$10^{11}\,\mathrm{cm}^{-2}$ generated in the system by the laser pulse. Self-consistent calculations considering the residual shallow donors and acceptors show that the residual carrier density ($n_0 + p_0$) in this system has the same order of magnitude. We, therefore, believe that the BR model describes accurately carrier dynamics in this system because of the relative magnitude between the optically generated carrier density ($\Delta n(t)$) and the intrinsic equilibrium carrier density ($n_0 + p_0$). In type-II optical transitions, due to the small oscillator strength, relatively high excitation powers are required to detect reasonable PL signals, thus generating higher relative carrier densities. In type-I systems, due to the large oscillator strength, the PL intensity is considerably stronger and low excitation powers are required to obtain measurable PL intensities. In this case, $n_0 + p_0$ is usually larger than $\Delta n(t)$, thus leading to an exponential carrier decay dynamics, as described by Equation (4).

Figures 4(c) and 4(d) show that, as the excitation power is increased, the fittings with Equations (5) and (6) agree for the first 700 ns due to the increased relevance of the $\Delta n^2(t)$ term. For comparison, Figure 4(c) also shows a fit employing the usual two-exponential approach (orange solid line). As we observe, the addition of a second decay constant does not yield satisfactory reproduction of the experimental data. However, again, better fit for the whole time range is found with Equation (6). Even varying the excitation power for more than 2 orders of magnitude, we verified that, for all measured powers, the values of τ obtained from the fit with Equation (6) are similar. Taking into account the results from all measured powers, we obtain average values of $\tau_{WL} = (0.40 \pm 0.05)\mu$s and $\tau_{QD} = (0.7 \pm 0.1)\mu$s for WL and QD emissions in sample C, respectively. The fact that $\tau_{QD} > \tau_{WL}$ is a consequence of the stronger confinement for QDs as compared to WL, which reduces average electron-hole wavefunction overlap. Moreover, the fact that τ is approximately constant for all excitation powers is consistent with the assumption that B is a constant in the derivation of Equation (6).

Figure 5(a) presents the values of $\Delta n_0/(n_0 + p_0)$ as a function of the excitation power obtained with Equation (7) after fitting the time transients of sample C with Equation (6). As we observe, even for the highest excitation powers, the carrier density generated by optical excitation in QDs and WL does not exceed a factor of 10 as compared to the residual carrier density. Since no significant variation in the values of τ_{QD} or τ_{WL} is observed in this power range, this is an indication that many-body effects can be neglected in our system under these experimental conditions. Figure 5(b) illustrates how the PL transient obtained from Equation (6), for a fixed $\tau = 0.4\,\mu$s, changes when the initial carrier concentration Δn_0 is increased by one order of magnitude. As we observe, increasing the initial carrier density leads to a faster decay (shorter transient) due to an increase in the contribution of the last term in Equation (3) for times immediately after laser excitation. This is consistent with the behavior observed for WL (Figures 4(a) and 4(c)) and QD

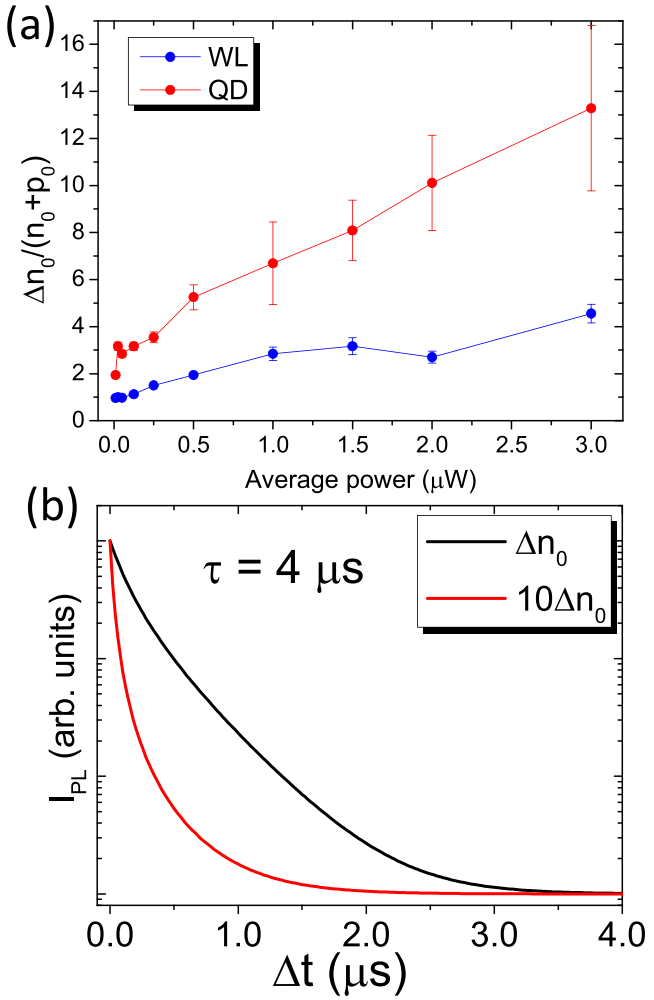

FIG. 5. (a) Ratio $\Delta n_0/(n_0+p_0)$ obtained from Equation (7), after fitting the time transients of sample C with Equation (6) for different excitation powers. (b) Plot of Equation (6) (normalized) for a fixed decay constant ($\tau = 0.4\,\mu s$) and two arbitrarily chosen carrier densities: $\Delta n_0 = 10^{11}\,cm^{-2}$ and $\Delta n_0 = 10^{12}\,cm^{-2}$, assuming $(n_0+p_0) = 10^{11}\,cm^{-2}$.

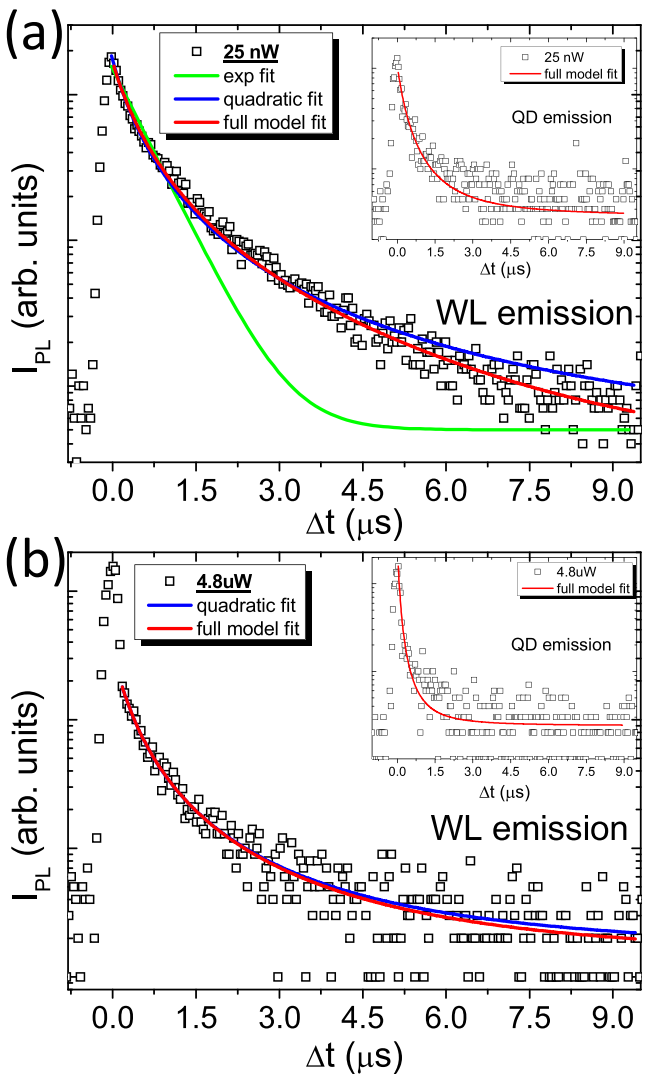

FIG. 6. PL intensity as a function of time from sample B for WL emission at (a) 25 nW and (b) 4.8 μW at 100 kHz. The insets show the transients for the QD emission. Solid lines represent fittings with Equations (4) (green), (5) (blue), and (6) (red).

emissions (Figures 4(b) and 4(d)) where the low power transients last longer than the high power ones.

The same fitting agreement with Equation (6) is obtained for sample B, as shown in Figures 6(a) and 6(b) for the WL emission. Note that in Figure 6(b), the high power (4.8 μW at 100 MHz) profile of the WL emission has a fast decay component. In this case, the fast decay appears due to the blue-shift of E^I_{WL} and the broadening of the E^D_{QW} peak in sample B which merge the two emissions as power is increased. At high powers we, therefore, start the fit only after a delay time when the QW emission is negligible. As power is decreased, this fast decay component disappears and the whole time range can be fitted with Equation (6), as demonstrated by the 25 nW transient shown in Figure 6(a). QD transients for high and low powers, fitted with Equation (6), are shown in the insets of Figures 6(a) and 6(b), respectively.

The fittings with Equation (6) of the transients from sample B provided average values of $\tau_{WL} = (3.3\pm0.5)\mu s$ and $\tau_{QD} = (5\pm2)\mu s$ for WL and QD emissions, respectively. In order to compare our results with others in the literature, it is important to remember that, since we use a single time constant, the values of τ lie somewhere in between the commonly used τ_1 and τ_2, but are usually similar to τ_2. To our knowledge, for GaSb QDs, τ_1 has not exceeded a few ns,[13,15,17,19,31] while the longest τ_2 value reported so far is 600 ns.[15] In our reference sample, $\tau \approx 8$ ns for the WL emission. The values of τ presented in Figure 6, therefore, demonstrate that the lifetimes obtained in our hybrid structures are among the longest ones reported for this system.

The effect of the electron-hole separation d is reflected on the lifetimes obtained for the E^I_{WL} transition in samples B and C. As we observe, the ratio between E^I_{WL} lifetimes in samples B and C is ≈ 8 because the larger value of d decreases electron-hole wavefunction overlap and, consequently, increases recombination times. In order to get a more quantitative understanding of this result, we calculated the electron-hole wavefunction overlap in the low power regime for the WL emission for the QW + WL hybrid system using envelope function approximation. We used a 5 nm thick GaAs QW and three monolayers of the GaSb WL. Since the recombination lifetime is proportional to the

inverse of the squared wavefunction overlap, we were able to estimate the ratio between WL lifetimes expected for samples B and C. The calculations predict values between 7 and 25, considering an uncertainty of 1 nm in the value of d, thus indicating that the experimental values are in reasonable agreement with theory.

IV. CONCLUSIONS

In summary, the results shown here demonstrate that growing a type-I GaAs QW at a chosen distance from type-II GaSb QDs is an interesting approach to engineer carrier wavefunction overlap and change exciton lifetimes in type-II systems. By comparing the carrier lifetime obtained for non-hybrid GaSb/$Al_xGa_{1-x}As$ QDs (our reference sample and previous reports in the literature cited in this work) with the ones obtained after the addition of a QW (sample B - $\tau_{QD} \approx 5\,\mu s$), we show that carrier recombination rates can be diminished by at least two orders of magnitude, which can be very interesting in the design of future charge memory devices.[11,12] Moreover, we demonstrated that, in our hybrid system, the optical emission transients are quite well described by the bimolecular recombination approximation. This model can be applied not only to study carrier recombination in other inorganic systems, but in organic ones as well. We, therefore, believe that this work can motivate further investigations and tests of the validity of this approximation.

ACKNOWLEDGMENTS

The authors would like to thank the São Paulo Research Foundation FAPESP (Grant Nos. 2012/11382-9 and 2014/17141-9), the Brazilian National Council for Scientific and Technological Development (CNPq), and CAPES for financial support.

[1]T. D. Ladd, F. Jelezko, R. Laflamme, Y. Nakamura, C. Monroe, and J. L. O'Brien, Nature **464**, 45 (2010).
[2]A. J. Shields, Nat. Photonics **1**, 215 (2007).
[3]A. Marent, M. Geller, A. Schliwa, D. Feise, K. Poetschke, D. Bimberg, N. Akçay, and N. Oncan, Appl. Phys. Lett. **91**, 242109 (2007).
[4]T. Nowozin, L. Bonato, A. Hoegner, A. Wiengarten, D. Bimberg, W. Lin, S. Lin, C. J. Reyner, B. L. Liang, and D. L. Huffaker, Appl. Phys. Lett. **102**, 052115 (2013).
[5]R. B. Laghumavarapu, A. Moscho, A. Khoshakhlagh, M. El-Emawy, L. F. Lester, and D. L. Huffaker, Appl. Phys. Lett. **90**, 173125 (2007).
[6]P. J. Carrington, A. S. Mahajumi, M. C. Wagener, J. R. Botha, Q. Zhuang, and A. Krier, Physica B **407**, 1493 (2012).
[7]P. J. Carrington, M. C. Wagener, J. R. Botha, A. M. Sanchez, and A. Krier, Appl. Phys. Lett. **101**, 231101 (2012).
[8]H. Fujita, P. J. Carrington, M. C. Wagener, J. R. Botha, A. R. J. Marshall, J. James, A. Krier, K. H. Lee, and N. J. Ekins-Daukes, Prog. Photovoltaics **23**, 1896 (2015).
[9]J. Tatebayashi, A. Khoshakhlagh, S. H. Huang, G. Balakrishman, L. R. Dawson, D. L. Huffaker, D. A. Bussian, H. Htoon, and V. Klimov, Appl. Phys. Lett. **90**, 261115 (2007).
[10]H. S. Hsu, W. C. Hung, C. C. Chang, W. H. Lin, M. H. Shin, P. T. Lee, S. Y. Lin, S. W. Chang, and Y. C. Chang, Appl. Phys. Lett. **107**, 091113 (2015).
[11]A. Marent, T. Nowozin, M. Geller, and D. Bimberg, Semicond. Sci. Technol. **26**, 014026 (2011).
[12]M. Hayne, R. J. Young, E. P. Smakman, T. Nowozin, P. Hodgson, J. K. Garleff, P. Rambabu, P. M. Koenraad, A. Marent, L. Bonato *et al.*, J. Phys. D: Appl. Phys. **46**, 264001 (2013).
[13]C. K. Sun, G. Wang, J. E. Bowers, B. Brar, H. R. Blank, H. Kroemer, and M. H. Pilkuhn, Appl. Phys. Lett. **68**, 1543 (1996).
[14]E. R. Glaser, B. R. Bennett, B. V. Shanabrook, and R. Magno, Appl. Phys. Lett. **68**, 3614 (1996).
[15]F. Hatami, M. Grundmann, N. N. Ledentsov, F. Heinrichsdorff, R. Heitz, J. Boehrer, D. Bimberg, S. S. Ruvimov, P. Werner, V. M. Ustinov *et al.*, Phys. Rev. B **57**, 4635 (1998).
[16]R. A. Hogg, K. Suzuki, K. Tachibana, L. Finger, K. Hirakawa, and Y. Arakawa, Appl. Phys. Lett. **72**, 2856 (1998).
[17]K. Gradkowski, T. J. Ochalski, N. Pavarelli, H. Y. Liu, J. Tatebayashi, D. P. Williams, D. J. Mowbray, G. Huyet, and D. L. Huffaker, Phys. Rev. B **85**, 035432 (2012).
[18]P. D. Hodgson, R. J. Young, M. A. Kamarudin, Q. D. Zhuang, and M. Hayne, Phys. Rev. B **88**, 155322 (2013).
[19]H. M. Ji, B. Liang, P. J. Simmonds, B. C. Juang, T. Yang, R. J. Young, and D. L. Huffaker, Appl. Phys. Lett. **106**, 103104 (2015).
[20]F. Qiu, W. Qiu, Y. Li, X. Wang, Y. Zhang, X. Zhou, Y. Lv, Y. Sun, H. Deng, S. Hu *et al.*, Nanotechnology **27**, 065602 (2016).
[21]P. D. Hodgson, R. J. Young, M. A. Kamarudin, P. J. Carrington, A. Krier, Q. D. Zhuang, E. P. Smakman, P. M. Koenraad, and M. Hayne, J. Appl. Phys. **114**, 073519 (2013).
[22]Y. I. Mazur, B. L. Liang, Z. M. Wang, D. Guzun, G. J. Salamo, Z. Y. Zhuchenko, and G. G. Tarasov, Appl. Phys. Lett. **89**, 151914 (2006).
[23]Y. I. Mazur, V. G. Dorogan, J. E. Marega, M. Benamara, Z. Y. Zhuchenko, G. G. Tarasov, C. Lienau, and G. J. Salamo, Appl. Phys. Lett. **98**, 083118 (2011).
[24]G. Moody, M. E. Siemens, A. D. Bristow, X. Dai, A. S. Bracker, D. Gammon, and S. T. Cundiff, Phys. Rev. B **83**, 245316 (2011).
[25]M. Superek, J. Andrzejewski, W. R. Rudzinski, G. Sek, J. Misiewicz, E. M. Pavelescu, C. Gilfert, and J. P. Reithmaier, Phys. Rev. B **85**, 125311 (2012).
[26]D. Guzun, Y. I. Mazur, V. G. Dorogan, M. E. Ware, J. E. Marega, G. G. Tarasov, C. Lienau, and G. J. Salamo, J. Appl. Phys. **113**, 154304 (2013).
[27]X. J. Yang, T. Kiba, T. Yamamura, J. Takayama, A. Subayo, K. Sueoka, and A. Murayama, Appl. Phys. Lett. **104**, 012406 (2014).
[28]A. Murayama, T. Asahina, K. Nishibayashi, I. Souma, and Y. Oka, Appl. Phys. Lett. **88**, 023114 (2006).
[29]R. B. Laghumavarapu, B. L. Liang, Z. S. Bittner, T. S. Navruz, S. M. Hubbard, A. Norman, and D. L. Huffaker, Sol. Energy Mater. Sol. Cells **114**, 165 (2013).
[30]S. Hatch, J. Wu, K. Sablon, P. Lam, M. C. Tang, Q. Jiang, and H. Y. Liu, Opt. Express **22**, A679 (2014).
[31]M. Sun, P. J. Simmonds, R. B. Laghumavarapu, A. Lin, C. J. Reyner, H. S. Duan, B. Liang, and D. L. Huffaker, Appl. Phys. Lett. **102**, 023107 (2013).
[32]M. Sopanen, H. Lipsanen, and J. Ahopelto, Appl. Phys. Lett. **66**, 2364 (1995).
[33]C. Obermueller, A. Deisenrieder, G. Abstreiter, K. Karrai, S. Grosse, S. Manus, J. Feldmann, H. Lipsanen, M. Sopanen, and J. Ahopelto, Appl. Phys. Lett. **75**, 358 (1999).
[34]L. Mueller-Kirsch, R. Heitz, A. Schliwa, O. Stier, D. Bimberg, H. Kirmes, and W. Neumann, Appl. Phys. Lett. **78**, 3908 (2001).
[35]M. Hayne, O. Razinkova, S. Bersier, R. Heitz, L. Mueller-Kirsch, M. Geller, D. Bimberg, and V. V. Moshchalkov, Phys. Rev. B **70**, 081302 (2004).
[36]K. Gradkowski, T. J. Ochalski, D. P. Williams, S. B. Healy, J. Tatebayashi, G. Balakrishnan, E. P. O'Reilly, G. Huyet, and D. L. Huffaker, Phys. Status Solidi B **246**, 752 (2009).
[37]D. Alonso-Alvarez, B. Alen, J. M. Garcia, and J. M. Ripalda, Appl. Phys. Lett. **91**, 263103 (2007).
[38]E. F. Schubert, *Light-Emitting Diodes* (Cambrige University Press, 2003).
[39]G. Lakhwani, A. Rao, and R. H. Friend, Annu. Rev. Phys. Chem. **65**, 557 (2014).